

Three-Dimensional Numerical Modeling of Confined and Unconfined Turbidity Currents – Model Development and Validation

Tarek M. Salah EL-Din^{1,*}, Serine A. Bashandy²

¹ Irrigation and Hydraulics Department, Faculty of Engineering, Cairo University, Giza, Egypt, email: tmsalahe2002@yahoo.com

² Irrigation and Hydraulics Department, Faculty of Engineering, Cairo University, Giza, Egypt, email: eng.serine.ahmed@gmail.com

*Corresponding author, DOI: 10.21608/PSERJ.2024.272754.1323,

ABSTRACT

Turbidity currents are sediment-laden gravity currents that transfer sediments to deep sea and lake floors through erosion and deposition. These deposits form subaqueous fans in deep marine environments and can reduce reservoir storage capacity, complicating management. Deep sea deposits often contain hydrocarbons like oil and gas. Field measurements of turbidity currents are challenging due to the risk of damage to measuring instruments, and laboratory experiments do not accurately simulate these currents. Thus, numerical modeling is crucial for understanding their formation and properties, and for locating oil and gas fields within deep sea turbidites.

A 3D two-phase numerical model (water and solids) is used to simulate underflow turbidity currents. This model solves the Reynolds-Averaged Navier-Stokes equations and uses the Eulerian approach, with turbulence closure achieved by the RNG k- ϵ model. It simulates both continuous unconfined currents and surge-like confined currents. Calibration and validation against experimental data show the model accurately replicates key features of turbidity currents.

Model results indicate that fine particles remain suspended longer, providing additional density that drives the current further with increasing downstream velocity. Vertical concentration profile shows two distinct layers: a denser, faster-moving bottom layer parallel to the bed, and a slower, more diluted upper layer affected by entrainment and mixing with ambient fluid. Turbidity currents are supercritical on sloped channels and subcritical on mild sloped unconfined seafloors or reservoir bottoms. In following article, hypothetical simulations using this model will further explore various characteristics and deposits of turbidity currents on a field scale.

Keywords: Turbidity Current, Submarine Fans, Multiphase Flow, Confined, Unconfined.

Received 31/3/2024

Revised 5/6/2024

Accepted 25/6/2024

© 2024 by Author(s) and PSERJ.

This is an open access article licensed under the terms of the Creative Commons Attribution International License (CC BY 4.0).

<http://creativecommons.org/licenses/by/4.0/>



1 INTRODUCTION

Turbidity currents are sediment laden gravity underflow currents that occur in different types of water bodies such as marine environment and freshwater reservoirs. These currents are characterized by their high sediment concentration, which increases the density of the water, causing it to flow down slope under the influence of gravity. They derive their propulsive force from suspended sediment. Gravity flows are caused by

differences in density between two fluids, typically caused by variations in temperature, salinity, and or the presence of suspended sediment. Turbidity currents exchange sediment with the bed of the channel by erosion and deposition, as flow travels downstream. This causes the density of the mixture surpassing that of the surrounding water, categorizing them as self-generated currents. When all suspended sediment is deposited on the bottom, the flow diminishes, and it rises when sediment is entrained from the bed into the suspension. They constitute a major

mechanism for the transport of sediment into deep sea floor and lakes bottom [1].

Turbidity currents arise from a variety of natural and man-made causes. Natural causes include various geological events such as submerged landslides, volcanic eruptions, earthquakes, slope failures, and oversteepening, the plunging of sediment-laden river flows during floods, and storm-induced erosion of canyon walls. Human activities may cause creation of turbidity currents in various ways. Disposing sediments into marine environment as a result of land reclamation as well as releasing industrial, chemical or municipal waste are common causes of turbidity currents.

Numerous aspects of turbidity currents' hydraulic behavior exhibit similarities to density currents generated by temperature and salinity differences. Whereas salt and heat are conservative pollutants, sediments lack this quality, because sediment can be either entrained from or deposited on the bed, affecting the overall quantity of suspended sediment. The sediment-laden water becomes turbid and the current is capable of eroding the seafloor, leading to the formation of submarine canyons which are usually characterized by steep slope and confinement. Turbidity currents dynamically interact with the surrounding water body by entraining clear, less dense water into the flow, in addition to engaging with its bed through sediment erosion and deposition processes. As the current travels, it continues to entrain sediment from the seafloor, which further increases its density and velocity, as depicted in Figure (1).

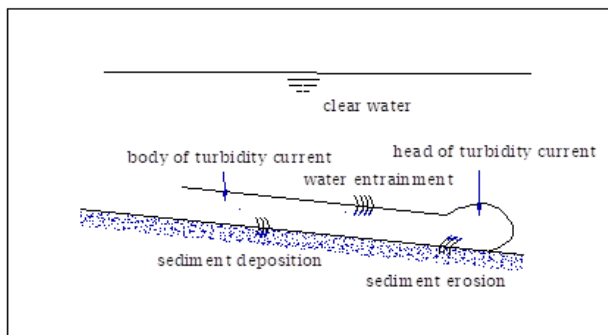


Figure 1: Definition sketch showing interaction of turbidity current with bed and clear water.

Upon reaching a region of lower gradient or a more quiescent environment, the current begins to decelerate, and the sediment it carries starts to settle out. This results in a graded bed of sediment, known as a turbidite, with the coarsest particles at the base and the finest at the top. In submarine environments, turbidity currents are able to change the morphology of continental slope through incision of channels (canyons) on steep slopes and deposit their sediment forming submarine fans on mild sea slopes. These turbidite deposits build up into vast sediment accumulations, which are source of hydro-carbon storage that usually contain oil and gas. Locating deep sea turbidites caused by turbidity currents events helps to locate oil and gas reservoirs in marine environment.

In reservoirs, turbidity currents are responsible for much of reservoir sedimentation, causing consequent loss of reservoir storage and may cause blocking of intake structures and sediment accumulation into hydropower plants. Very fine sediment particles transported into reservoirs can also increase turbidity levels and thus deteriorate water quality [1].

Turbidity currents are classified into two types according to their origin and cause: discontinuous or surge-like currents and continuous or plume-like currents. Discontinuous currents are typically resulted from instantaneous sources of suspended sediment and are thus short-lived phenomena. Earthquakes cause most of discontinuous turbidity currents. Continuous currents, on the other hand, are produced by consistent sources of suspended sediment and can endure for hours or even days. Continuous turbidity currents are distinguished by a body that is several times longer than the length of the head, whereas surge-like or discontinuous currents have a body that is similar to the length of the head. The turbidity current vertical velocity profile can be divided into two sub-regions. The division is the place of greatest velocity. The concentration profile can be linear in the upper area of the flow and comparable to sediment distribution in open channel flow in the lower region. Turbidity currents can also be classified according to the passage they move into. Turbidity currents can be confined while flowing in steep slope confined submarine canyons and they become unconfined when enters the mild slope open deep sea floor where no boundaries exist to limit their extension in both horizontal directions.

1.1 PROBLEM DEFINITION AND CURRENT STUDY OBJECTIVE

Occurrence of turbidity currents are rare to observe and difficult to study in the field due to their unpredictable occurrence. Field measurements are difficult and expensive to conduct. In deep water in marine environment or reservoirs, even weak turbidity currents may damage or move measuring instrumentation especially those close to the bottom [1], [2]. Field investigations are mostly limited to the examination of deposits formed by previous turbidity currents events [1], [2]. On the other hand, laboratory experiments provide an alternate way for simulating and studying the dynamics of turbidity currents. Laboratory experiments can be useful to investigate the flow field and sediment concentration characteristics, however, studying turbidite deposits is not possible through laboratory experiments. Also, experimental approaches cannot be used to simulate all practical situations. Utilization of experimental studies is limited by the large number of required data, inaccuracies in these data and the difficulties to represent all field conditions in laboratory experiments.

Analytical and numerical solution may present an efficient and cost-effective method to study turbidity currents characteristics and the associated formed

turbidite deposits. Analytical and numerical models can provide reasonable and accurate representation about the formation and characteristics of turbidity currents and their turbidite deposits. Most of numerical research is based on one of two approaches. The first approach is the single-phase vertically averaged equations of motion, as demonstrated by Imran and Parker [3]. In the study by Michele and Allen, [4], they found that the gravity current follows shallow wave phenomenon in which the gravity current's lengthwise spread (L) is significantly greater by an order of magnitude than its depth (h). The second numerical approach solves complete equations of motion to simulate turbidity current dynamics either by Direct Numerical Simulation (DNS) or Large Eddy Simulation (LES). DNS solves Navier Stokes equations with no consideration of turbulence model solving all turbulent eddies. LES solves large eddies and minor eddies are modelled separately. Due to the intensive computational demands, Direct Numerical Simulation (DNS) and Large Eddy Simulation (LES) are typically restricted to analyzing flows that have low Reynolds numbers within simplified geometries.

The current research utilizes a two-phase technique to solve Reynolds-averaged Navier-Stokes equations, supported by a validated turbulence closure scheme. The present research targets to develop and validate a robust numerical model that simulate 3D turbidity currents using the available CFD package. The model is capable of simulation continuous or surge like turbidity currents either confined (when flow into steep slope channel which can be submarine canyon) or unconfined (when spreads over mild slope sea floor). The model also can predict the turbidite deposits associated with the turbidity current. Model accuracy and ability to simulate turbidity currents flow characteristics are validated by comparison of the numerical results with two sets of authenticated laboratorial results available in literature of continuous unconfined turbidity current and surge like decelerating depositional confined turbidity current. In extended future research, further investigation of the flow characteristics (flow field, concentration distribution, turbulence characteristics) of both types of turbidity currents shall be performed through hypothetical simulations to be performed by the developed model on the field scale.

1.2 PREVIOUS EXPERIMENTAL STUDIES

Since field measurements of turbidity currents are difficult to conduct and requiring under water work with special equipment which are most probably subject to destruction by currents, researchers have utilized laboratory experiments to investigate the behavior of turbidity currents. Laboratory results were used to deduce empirical formulas which are limited in application. Also, their applicability to real turbidity currents is questionable since there are no field measurements to compare with. Experimental studies on turbidity currents have been

reported and documented in the literature focusing on either continuous unconfined turbidity current and on surge like decelerating depositional confined turbidity current.

Gladstone, et al.[5], performed laboratory experiments on surge like decelerating depositional confined turbidity current. They investigated two-dimensional constant-volume gravity currents with bi-disperse and multi-disperse grain size distribution. They utilized the experimental results to develop some empirical equations representing features of confined surge like turbidity current. They conclude that, the fractions of different sediment sizes strongly affect both the motion of the currents and the sedimentation pattern. Introducing a minor proportion of fine sediment into a coarse-grained turbidity current significantly affects the current's velocity, extent of spread, and patterns of sediment deposition, to a greater extent than the addition of a small quantity of coarse sediment does to a fine-grained gravity current.

Flelix and Peakail [6], conducted three sets of lock exchange experiments to study the transformation of debris flows into turbidity currents. They concluded that debris flows, which are initially highly dense and viscous, experience only superficial changes, leading to the formation of a weak turbidity current. In flows that initially less dense and viscous, the transformation is more profound, affecting the entire flow domain and causing all sediment material to be incorporated into the resultant turbidity currents.

Baas et al.[7] performed several laboratory experiments representing the flow of continuous hyperpycnal turbidity current that initially move confined in subaqueous mild slope channel and then spreads over horizontal or mild slope unconfined submarine fan. The experimental model consisted on sloped confined channel ends with horizontal wide basin. Sediment water mixture with different composition and concentration were released at the upper end of the sloped channel with different roughness. Experiments were also performed using different mild and steep channel slope. Subaqueous fans were created and measured, and the sedimentation pattern was investigated against different controlling parameters.

Kyle M. Straub [8], Conducted laboratory experiments to investigate the interactions between turbidity current and aggrading sinuous channel. The study concluded that the asymmetry of over bank sedimentation at bends was related to bend induced cross channel flow. The high super elevation measured in the experimental bends is a combination of centrifugal contribution and a run up associated with the momentum of a current.

Remo Cossu and Mathew G. Wells [9], performed a series of lock-release experiments to investigate shear stresses and turbulent kinetic energy distribution within weakly depositional turbidity and saline density currents. Maximum positive Reynolds stresses appear when the flow velocity gradient is largest in the bottom boundary layer but decrease significantly below this peak value.

Hill and Lintern [10], studied field measurements of 12 events of unconfined turbidity currents on the Fraser delta slope collected using Acoustic Doppler Current Profiler. The observation that only about half of the flows measured at the shallower site are detected at the deeper site implies that the runout distances of open slope flows are restricted. Weaker flows exhibit minimal differences in speed and direction compared to ambient tidal velocities. The flow directions indicate that these open slope flows are unconfined and originate in the upper slope region. Shallow gullies play a crucial role in initiating and igniting flows that subsequently become unconfined on the lower part of the slope.

Guimarães et al. [11], studied experimentally the depositional behavior of three-dimensional unconfined turbidity currents performed in a large-scale channel-basin tank without slope break. Two flow rate models with different hydrodynamic characteristics and two distinct lobes have been identified from the experimental results. Lower flow rates and velocities resulted in elongated lobate deposits with downstream sediment fining. Higher flow rates and velocities produced radial and downstream fining sediment with ripples and dunes.

Liu et al.[12] defined the relationship between the ambient fluid and the turbidity current through analysis of many field observations, laboratory experiments as well as numerical simulation results collected and surveyed from 806 previous articles. The behavior and properties of turbidity currents and their interactions with the ambient fluid is mainly influenced by not only the initial conditions but also the type and properties of the runout environment. Most of previous studies in literature focused on investigating the initial conditions while less and minor attention were given to the type and properties of the runout environment.

1.3 PREVIOUS NUMERICAL STUDIES

In the previous numerical studies, the turbidity current governing equations were defined. Some studies conducted numerical models based on three equations describing the mass balance of fluid, mass balance of sediment and the momentum of the flow. Subsequent research incorporated the mean turbulence energy equation, imposing a limitation on the feasible solutions for the three-equation model. This is because the sediment uptake from the bed is correlated with the turbulence intensity, as described in the four-equation model. The governing equations were solved using suitable numerical solution scheme to estimate the equations describing the under-flow parameters. The conducted models are usually verified against sets of field or laboratory measurements before application.

Bonnecaze, et al.[13], studied fixed volume particle-driven gravity currents released into lighter ambient fluid theoretically and experimentally. They constructed two numerical one-dimensional flow model based on shallow water equation of motion.

Garcia [14], conducted a depth-averaged model for neither steady non uniform turbidity current with well graded sediment. The model was developed by deriving three equations presented in layer-averaged form. The used equations were the fluid mass, the sediment mass and momentum balance.

Salahedin, et al.[15], developed one dimensional numerical model to simulate poorly sorted sediment laden turbidity current and the evolution of a Submarine Fan. The model was four equations model which conservation of water, sediment, momentum and turbulent Kinetic energy balance. The model was applied to a 50 km long of the Amazon Submarine Channel with different fractions and different fine sediment sizes. The model result indicated that an increase in the fraction of fine sediment dramatically increases the sand carrying capacity of the turbidity current allowing the current to preserve its momentum for long distances and transfer more sediments in the downstream direction.

Cesar, et al.[16], Developed 3D numerical model to simulate turbidity currents occur a reservoir due to river inflow. The governing equations used in the model were the incompressible Navier Stokes equations: continuity and momentum equations with additional equation for sediment concentration. The eddy viscosity was determined using the K- ϵ turbulence closure model. User defined sediment settlement and erosional equations were added to describe the sediment exchanges between flow and bed. The numerical model was validated with field and laboratory measurements. The results showed that turbidity current caused by a large flood entrains large sediment and transport this sediment for longer distances. They concluded that, the numerical model can be used to evaluate reservoir management.

Hall and Meiburg [17], Implemented Large Eddy Simulation (LES) into a turbidity current flow model. Large Eddy Simulation LES resolves the large scales of the flow. A sub grid model is conducted to account for the small scales using eddy viscosity (and diffusivity) model. The findings concluded that LES can replicate specific detailed flow characteristics, not merely the overall properties. Further examination of the flow's sedimentation and re-suspension features is necessary to thoroughly evaluate the effectiveness of LES. It can be a useful tool when performing 3D simulation and thus allowing to study the properties of 3D turbidity currents over complex boundaries in geophysical suitability.

Singh [18], conducted 3D numerical model solving depth-averaged Navier Stoke equations with the Boussinesq Approximation and mass balance of sediment equation as LES model. Modified Smagorinsky model was used for turbulence closure and the model constants C_s Smagorinsky constant, S_{ct} the Schmidt turbulence number were determined using reported experimental data. Model results were compared with reported data of 3D laboratory experiments. The model can predict complex 3D characteristics of turbidity current with reasonable accuracy for various complex conditions.

La Rocca and Pinzon [4] conducted 2D depth averaged mathematical model by derivation of the shallow water equations for conservative and non-conservative density currents. Concerning with the conservative density case, the 2D mathematical model accounted for the two superimposed liquid layers and the pressure at the upper surface. Concerning with the non-conservative density currents (Turbidity currents) the motion of the upper layer of liquid was neglected as it was assumed to have infinite depth, consequently the upper surface pressure was also neglected. A 3D full depth lock exchange experiment was performed to validate the mathematical models.

Strauss and Glinsky [19] applied nonlinear simulations to turbidity currents flowing down a slope and over an obstacle. The mathematical model was based on 2D depth dependent Navier – Stokes equations including poly disperse particles in the current and the substrate. The obstacle on the slope was used only to trigger development of sediment waves. They investigated the effect of four parameters on the generation of sediment waves: slope, current height, grain concentration and particle diameters. They determined that the creation of sediment waves is due to the interaction between the flow and the lower boundary condition. This intricate boundary condition alters the bottom topology via deposition of particles and the resuspension of particles from the substrate. An increased slope on the downstream side amplifies the flow's kinetic energy, which in turn escalates the resuspension by augmenting the shear stress. The overall effect is an increase in erosion. This erosion into the substrate results in a subsequent decrease in slope. Consequently, the flow's kinetic energy decreases, leading to an increase in deposition.

Georgoulas, et al.[20], proposed a 3D two-phase flow numerical model that simulates the motion and flow structure of turbidity currents. The numerical model utilized two-phase modification of Reynolds Averaged Navier-Stokes equations (RANS). Mass and momentum conservation laws are solved individually for each phase and then coupled through pressure and interphase exchange coefficients. RNG K- ϵ turbulent model is used for turbulence closure. They reproduced two previously published different series of laboratory experiments on turbidity currents in order to prove the capability of the numerical model to capture various characteristics of turbidity currents. They observed that the numerical simulation showed a good match with experimental data. They concluded that turbidity currents flow is highly sensitive to any change in the flow properties and that the numerical model is suitable for further examination of dynamic characteristics of turbidity currents.

Lesshaft et. al,[21] introduced a general formulation to predict the initial conditions of turbidity currents whose terminal deposition pattern match known data at specified locations. The performance of the developed procedure was assessed with a direct numerical simulation and a physical test. The numerical model was governed by 2D Navier-stokes equations using the Boussinesq

approximation. Sediment concentration is modeled according to an Eulerian convection-diffusion equation. The developed procedure reconstructs a given full deposit profile by performing iterative optimization that gives suitable initial conditions for the flow to simulate the given depositional pattern.

Serchi, et al.[22], performed 2D numerical model to study the turbidity currents based on Reynold averaged Navier-stokes equations. K- ϵ model was used to represent Reynolds Stress. Solution was performed using CFD software FLUENT 6.3.

An and Julien, [23], investigated detailed analysis of turbidity currents dynamics in Imha reservoir in south Korea using FLOW-3D (CFD) code. They applied Reynolds averaged Navier Stokes (RANS) equations with the (RNG) K- ϵ turbulence model. A new particle dynamic algorithm was devised and integrated with the FLOW-3D model to simulate the settling of various grain sizes. The accuracy of the model was confirmed through field measurements. The simulations results show that for low sediment concentrations, interflow is created while for high sediment concentrations, underflow turbidity current is formed. study showed that model provided very good predictions of temperature and sediment concentration.

Albertao et al. [24], utilized the Cellular Automata (CA) modeling technique to simulate turbidite flow deposits resulting from turbidity currents. The CA modeling incorporates the main submarine physical processes such as water entrainment, erosional and depositional processes. The CA modeling was applied to a real case (an oilfields of the Campos Basin offshore Brazil). The model reproduced sedimentation patterns, such as successive filling of contiguous sub-basins, increasing flow velocities in confined settings, run-up effects with lateral deposition of fines and concentration of coarser sediments in topographic lows. The results of the simulations are consistent with the geological model of the study area and predict reservoir distribution.

Traer et al. [25], expanded the one-dimensional, four-equation numerical model for turbidity currents to account for flow stripping and overspill effects. They found that, turbidity currents may reach an equilibrium state between the entrained mass (water and solid particles) and the mass lost to stripping and overspill, leading to uniform flow conditions. The equilibrium condition can assist to explain the long runout distances of subcritical turbidity currents on mild slopes. The model helped to understand the formation and behaviour of turbidity current evolution from submarine canyons to depositional fans.

Hu and Li [26] presented a layer averaged numerical model to solve the confined turbidity currents using combined approach of local graded-time-step and the global maximum-time-step. Finite volume method was used to solve unstructured triangular mesh. Numerical solution results showed reasonable agreement when compared to experimental results of the current head and turbidites profiles as well as field results of the current

head. The layer averaged model can reduce the simulation time and cost by up to 80%.

Naruse and Nakao [27] developed an inverse model to deduce turbidity currents flow characteristics from the characteristics of the deposits and turbidites caused from these previous currents. The inverse model is developed from forward one-dimensional model and neural networks approach. The model solved surge-type turbidity currents but modified to consider sediment transport and deposition of multiple grain size classes. The inverse model was tested on the field scale and found to be sufficient enough to reproduce the characteristics of turbidity currents events related to specific deposits and turbidites.

Rakesh et al. [28], studied the sediment transport and deep sea turbidites formation in submarine environment due to turbidity currents using multiphase approach solved by finite volume CFD solver. The model solved two phase flow of solid and water phases treated as an interpenetrating continuum. The model solved only the unconfined turbidity current in deep marine mild slope part without considering the guiding confined channel. They found that, the sediments still deposit while the current head is not decelerating, and they called it as slumping action. The study models the sedimentary process in a subaqueous medium based on gravity and density variations and subsequent quantitative analysis of turbidite deposits.

Zhang et al. [29], conducted sensitivity analysis to determine the optimal numerical model configuration for accurately simulating the characteristics of turbidity currents. These currents were simulated using a three-dimensional numerical model, which incorporated domain discretization, a turbulence closure model, and a transport scheme.

2 NUMERICAL MODELLING DEVELOPMENT

ANSYS 2023 R1 is employed to solve the governing equations using the finite volume method. An implicit formulation is selected to convert the discretized equations to linear equations for the dependent variables in all computational cells in the domain. The suggested CFD model based on 3D two-phase numerical technique for the modelling of turbidity current motion and depositional features using RNG k- ϵ turbulence model for turbidity current flows with low Reynolds numbers. Ansys can be used to simulate turbidity currents with poorly sorted sediment content which are more similar to natural turbidity currents either diluted or dense.

Turbidity currents consist of a primary water phase and secondary suspended sediment phase scattered within the water phase. The proposed model uses a two-phase technique to solve Reynolds-averaged Navier-Stokes equations as well as the Eulerian model. For each phase, it solves a set of momentum and continuity equations. Eulerian model relates between phases in a four-way

relation in which the water phase dominates sediment phase via drag and turbulence transfer. Coupling between phases is a four-way interaction in which the fluid phase dominates the motion of the particles phase through drag and turbulence transmission. In the fluid phase, the particle phase reduces mean momentum and turbulence. The interphase exchange coefficients provide the coupling. The computational model employs the RNG k- ϵ turbulence model, which provides greater accuracy for swirling flows and rapidly strained flows. The computational model utilized finite volume method. Therefore, it is suitable for solving turbidity currents with complex geometries formed in reservoirs and marine environment where morphological abnormalities exist.

The Eulerian model also allows for the simulation of two or more interpenetrating fluids (or phases). A variable is introduced for each successive phase added to the model: volume percentage of the phase in each computational cell which should add to unity for all phases in each cell.

The model governing equations as solved by ANSYS are presented for multiphase flow. The Continuity equation can be written as follow for multiphase flow:

$$1/\rho_{rq} \left(\frac{\partial(\alpha_q \rho_q)}{\partial t} + \nabla \cdot (\alpha_q \rho_q \vec{v}_q) \right) = 0 \quad (1)$$

Where, \vec{v}_q is the velocity of the q^{th} phase and ρ_{rq} is the reference density, or the average density of the q^{th} phase all over the volume in the solution domain given as follows:

$$\rho_{rq} = \sum \alpha_q \quad (2)$$

The momentum conservation of the fluid q phase is:

$$\frac{\partial(\alpha_q \rho_q \vec{v}_q)}{\partial t} + \nabla \cdot (\alpha_q \rho_q \vec{v}_q \vec{v}_q) = -\alpha_q \nabla p + \nabla \cdot \bar{\tau}_q + \alpha_q \rho_q \vec{g} + \sum_{s=1}^n (K_{sq} (\vec{v}_s - \vec{v}_q)) + (\vec{F}_q + \vec{F}_{\text{lift},q}) \quad (3)$$

The momentum conservation of the solid S phase is:

$$\frac{\partial(\alpha_s \rho_s \vec{v}_s)}{\partial t} + \nabla \cdot (\alpha_s \rho_s \vec{v}_s \vec{v}_s) = -\alpha_s \nabla p - \nabla p_s + \nabla \cdot \bar{\tau}_s + \alpha_s \rho_s \vec{g} + \sum_{s=1}^n (K_{qs} (\vec{v}_q - \vec{v}_s)) + (\vec{F}_s + \vec{F}_{\text{lift},s}) \quad (4)$$

Where, K_{sq} is the interphase momentum exchange coefficient, \vec{v}_s is the solid phase velocity P is the static pressure, $\alpha_s \rho_s \vec{g}$ is the gravitational body force, p_s is the solid pressure, \vec{F}_q is the external body force, and $\vec{F}_{\text{lift},q}$ is the lift force. The stress-strain tensor $\bar{\tau}_q$ and $\bar{\tau}_s$ of phases q and S calculated by the following equations:

$$\bar{\tau}_q = \alpha_q \mu_q \left(\nabla \vec{v}_q + \vec{v}_q^T \right) + \alpha_q \left(\lambda_q - \frac{2}{3} \mu_q \right) \nabla \cdot \vec{v}_q \bar{I} \quad (5)$$

$$\bar{\tau}_s = \alpha_s \mu_s \left(\nabla \vec{v}_s + \vec{v}_s^T \right) + \alpha_s \left(\lambda_s - \frac{2}{3} \mu_s \right) \nabla \cdot \vec{v}_s \bar{I} \quad (6)$$

Where, μ_q and μ_s are the shear viscosities of phases q and s, λ_q and λ_s are the bulk viscosities of phases q and S, and \bar{I} is the identity tensor.

The shear tensor of the solid phase $S \bar{\tau}_s$ contains shear viscosity and bulk viscosity caused by particle movement and collision causing momentum exchange of the sediment particle. The model also includes a frictional aspect of viscosity to account for the transition from viscous to solid that takes place when the particles of a solid phase attain the maximum volume fraction of the solid.

In the current numerical solution, the Renormalization-group (RNG) $k-\epsilon$ model is utilized to account for turbulence. It is appropriate for turbidity currents modeling due to its accuracy in simulating swirling and rapidly strained flows. When the primary-phase turbulence significantly influences the random motion of the secondary phases, the dispersed turbulence model becomes the model of choice. The RNG $k-\epsilon$ model, enhanced with additional terms accounting for interphase turbulent momentum transfer, is used to make turbulent predictions for the continuous phase. Consequently, the fluctuating quantities of the secondary phases can be expressed in relation to the average characteristics of the primary phase and the ratio of particle relaxation time to eddy-particle interaction time. The modified RNG $k-\epsilon$ model for multiphase flow is used to obtain turbulent predictions.

3 NUMERICAL MODEL CALIBRATION AND VALIDATION

The proposed numerical model is calibrated and validated by reproducing previously published laboratory experiments. The results obtained from the model are compared to the previous experimental results to test the ability of the model to simulate the turbidity current with reasonable accuracy.

Laboratory experiments representing the flow of continuous unconfined turbidity current (conducted by Baas et al.[7]) and laboratory experiments representing the flow of surge like confined turbidity current (conducted by Gladstone et al.[5]) are simulated by the developed numerical model using the same initial conditions. Quantitative experimental results from the previous two studies are compared with the corresponding numerical results of the current study. Vertical velocity profiles for subcritical and supercritical flows produced in the work of Garcia [14] are used in both numerical runs to verify the flow vertical structure.

3.1 Validation with Experimental Results of Continuous Unconfined Turbidity Current

Figure (2) illustrates the geometry of the laboratory experiments to be simulated in this study as well as the generated mesh and the proposed boundary conditions.

The computational domain was divided into two zones. The first zone simulates the thick layer of loose sand layer while the second zone simulates the stagnant water

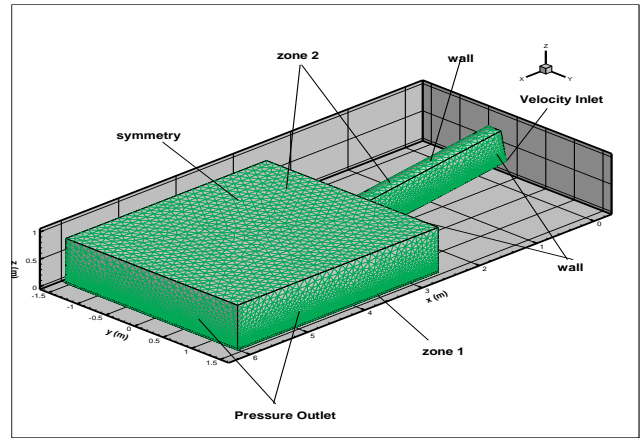


Figure 2: Mesh, geometry and boundary conditions used in numerical model simulating (Bass et al.[7]) experiments.

occupying the sloped channel and the ambient water above the loose bed layer.

The lock gate model assumes a zero-thickness gate, which does not account for the acceleration phase of lock release turbidity current development. At the gate, velocity inlet boundary condition was used to define the water and sand velocity magnitude and direction entering the channel, water turbulence parameters, sand volume fraction are also assigned at the inlet. The downstream outlet boundary condition is assumed as pressure outlet

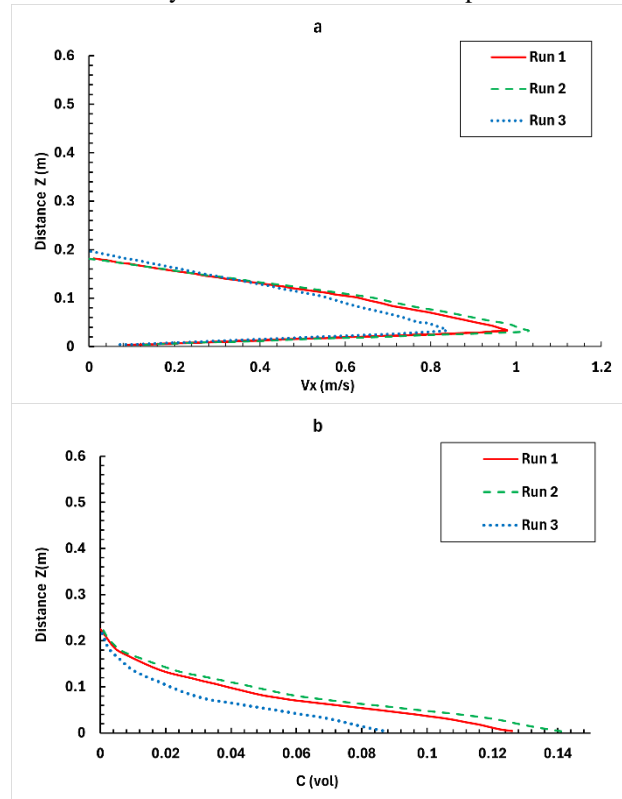


Figure 3: x-velocity profiles; a) Vertical volumetric concentration profiles, b) Vertical concentration profiles for numerical simulations 1,2, and 3 at $x=2.5m$, $y=0m$, and $t=15sec$

boundary condition. The static pressure on the ambient water is taken into account by a user defined function.

Table (1) shows the values of the mean height and dense layer thickness of the turbidity current for the experimental and numerical results for different initial concentrations for numerical simulations 1, 2, and 3. The numerical results are close to the experimental observed values.

Table 1. Comparison of numerical model results (present study) and (Baas et al [7]) experimental values for the average height and turbidity current layer thickness.

Numerical simulations	Initial sediment volume	Experimental Mean height of T.C. (m)	Experimental Dense layer thickness (m)	Numerical Mean height of T.C. (m)	Numerical Dense layer thickness (m)
1	0.27	0.24	0.12	0.19	0.13
2	0.35	0.18	0.14	0.19	0.15
3	0.14	0.24	0.11	0.2	0.14

The average height and turbidity current layer thickness is measured at the end of the quasi-steady discharge phase where the suspended sediment concentration as well as the current velocity diminish (become close to zero) or suddenly change slope as illustrated in Figure (3).

In numerical simulations 1, 2, and 3, the velocity time series of turbidity currents are plotted for a point at $x=0.6$ m, $y=0$ m, and $z=0.3584$ m, which corresponds to the location of the propeller type current meter in Baas et al [7] experience work. Figure (4) shows the head velocity of each numerical simulations, and Figure (5) shows the relationship between head velocity and turbidity current concentration.

Figure (4) demonstrates that the head velocities of all numerical simulations are smaller than the velocity of the current body, owing to the constant supply of faster fluid from the mixture pumped through the inlet gate to the current body. Figure (5) illustrates that turbidity head velocity is related to current concentration because sediment concentration increases buoyancy flux and thus current momentum.

Garcia's (1994) experimental work is used to validate the vertical structure of the turbidity current. Dimensionless vertical velocity profiles are created. The average velocity is used to normalize the streamwise

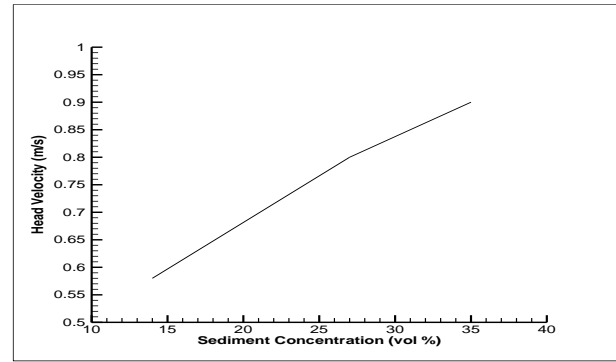


Figure 5: Relationship between turbidity current head velocity and sediment concentration from numerical simulations

velocity component, while the turbidity current height is used to normalize the vertical distance. The current study velocity profile is compared to the matching dimensionless velocity profile from Garcia's [14] experimental work, as shown in Figure (6).

Figure (6) indicates that, apart from the near bottom boundary, the model numerical results reasonably agree with Garcia's [14] experimental results. This is owing to the use of typical wall functions near the bottom boundary, which do not clarify, but rather connect the viscosity close to the wall with the region that is fully turbulent outside. Consequently, it can be concluded that the numerical model developed in the present study fairly simulates the continuous unconfined turbidity current.

From the numerical simulations of the present study simulating Baas et al. [30] laboratory experiments it can be noticed that the continuous unconfined turbidity current passes a discrete head, two unique body layers, and two velocity layers. The lower layer at the bottom of the flow moves more rapidly than the upper layer due to its denseness. Turbidity currents are supercritical in inclined channels and subcritical at the basin's end.

Because of horizontal spreading, the thickness of turbidity currents develops gradually inside confined channels and then reduces abruptly at the entry of unconfined basins. The thickness increases where the flow experiences an internal hydraulic leap. The fan-shaped geometry of sediment bodies generated by turbidity currents expanding in the basin is composed of a channel levee system connected to a lobe. These characteristics are depicted in the figures 7 to 13.

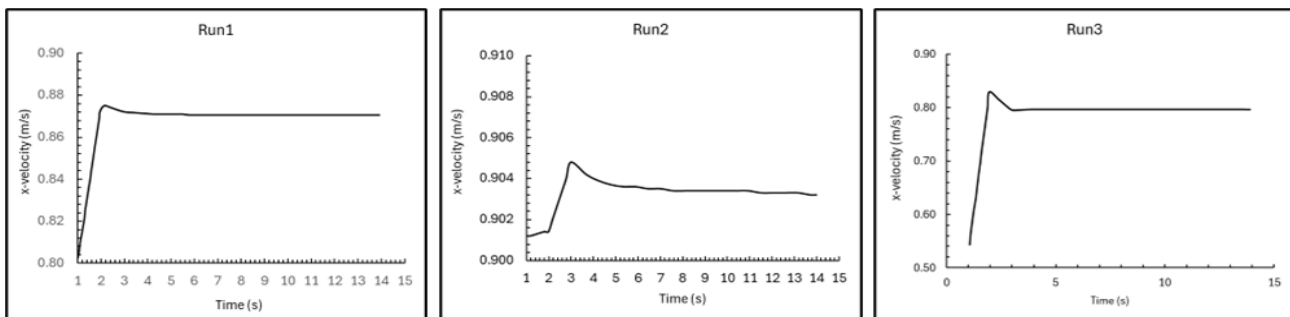


Figure 4: Velocity time series for numerical simulations 1, 2, and 3

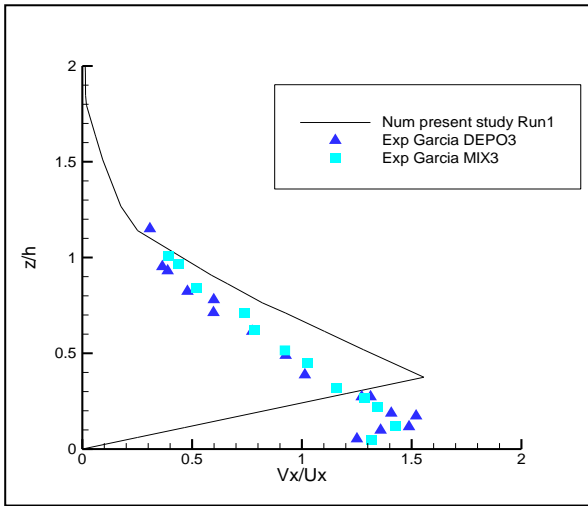


Figure 6: Comparison of numerical dimensionless velocity profile (present study) and experimental model (Garcia 1994) at $x=3.3$ m, $y=0$ m, and $t=45$ sec

3.2 Validation with Experimental Results of Surge Like Confined Turbidity Current

The numerical simulations utilize developed geometry, mesh, and boundary conditions as depicted in Figure (13) which represents a surge-like confined turbidity current.

Enhanced wall treatment approach is utilized in the present study in which the domain is subdivided into the region affected by viscosity and a fully turbulent region, based on a turbulent Reynolds number that depends on the distance from the wall. In viscosity affected region, ϵ and turbulent viscosity are obtained from algebraic equation, while in the full turbulent area, the RNG $k-\epsilon$ model is utilized.

The turbidity current front velocities provided in Gladstone et al. [5] experiments A, D, and G, are compared to the equivalent current numerical results by plotting front position vs time Figure (14). The numerical simulations results show good agreement with the previous experimental data. The simulation results reveal variations in the progression of the turbidity current front among the simulations produced, depending on the ratios of large and small sediment particles used in the initial suspension. All numerical curves begin with a steep part that lasts up to 20 seconds before gradually becoming less severe. The initial steep slope segment is associated with the recession stage of the turbidity currents, in which the current flow front remains essentially unchanged. The subsequent section of the curves shows consistent reduction in velocity, caused by the ongoing deposition of particles and the consequent decrease in excess density which is the primary driving agent of the currents.

The validity of the vertical structure of the turbidity current is examined against the experimental work of Garcia et al.,[14]. Vertical velocity profiles are constructed in dimensionless form. The streamwise velocity component is normalized with average velocity and the vertical distance is normalized with the turbidity current layer thickness.

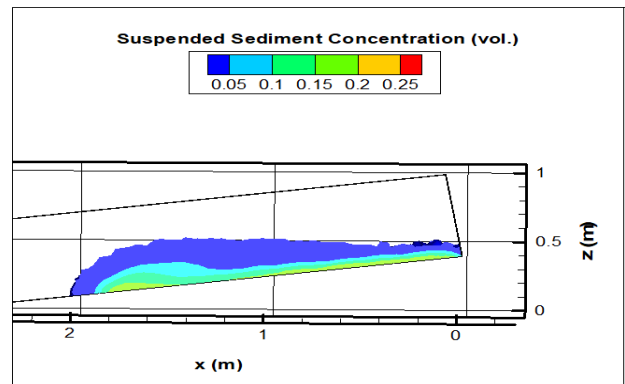


Figure 7: Suspended Sediment Concentration contours for numerical simulation 1, at time=3 sec, ZX section at $y=0$ m

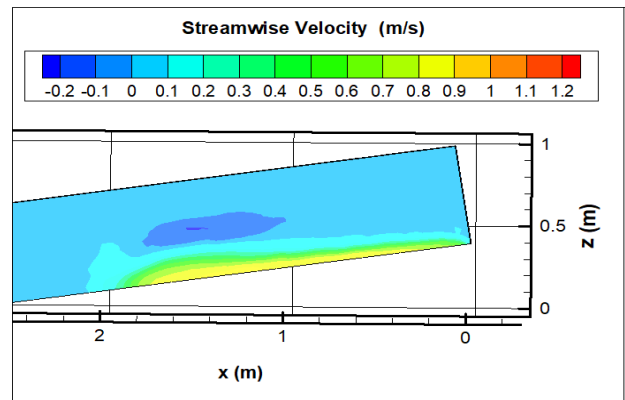


Figure 8: X-Velocity contours for numerical simulation 1, at time=3 sec., ZX section at $y=0$ m

The velocity profiles from the current numerical simulations are compared with the corresponding dimensionless velocity profile from the experiments of Garcia et al.[14] and the numerical results of Geogroulas et al.,[20] as illustrated in Figure 15. It is evident that the numerical dimensionless velocity profiles fall reasonably agree with the dimensionless velocity profiles for subcritical flow in the experimental work of Garcia et al. [14]. Consequently, it can be concluded that the numerical model developed in the present study fairly simulates the surge like confined turbidity current.

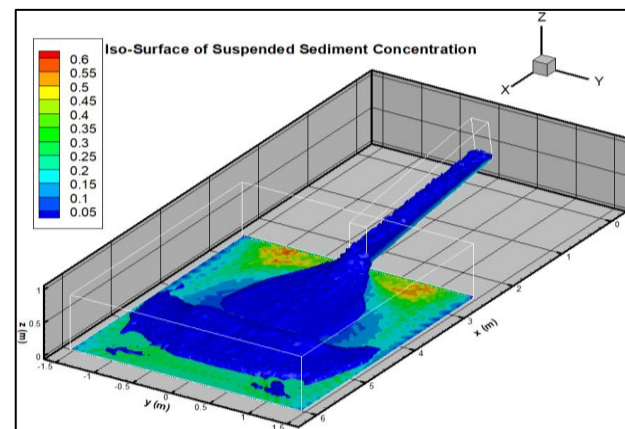


Figure 9: Iso-surfaces of suspended sediment concentration for numerical simulation 1, at time=15 sec

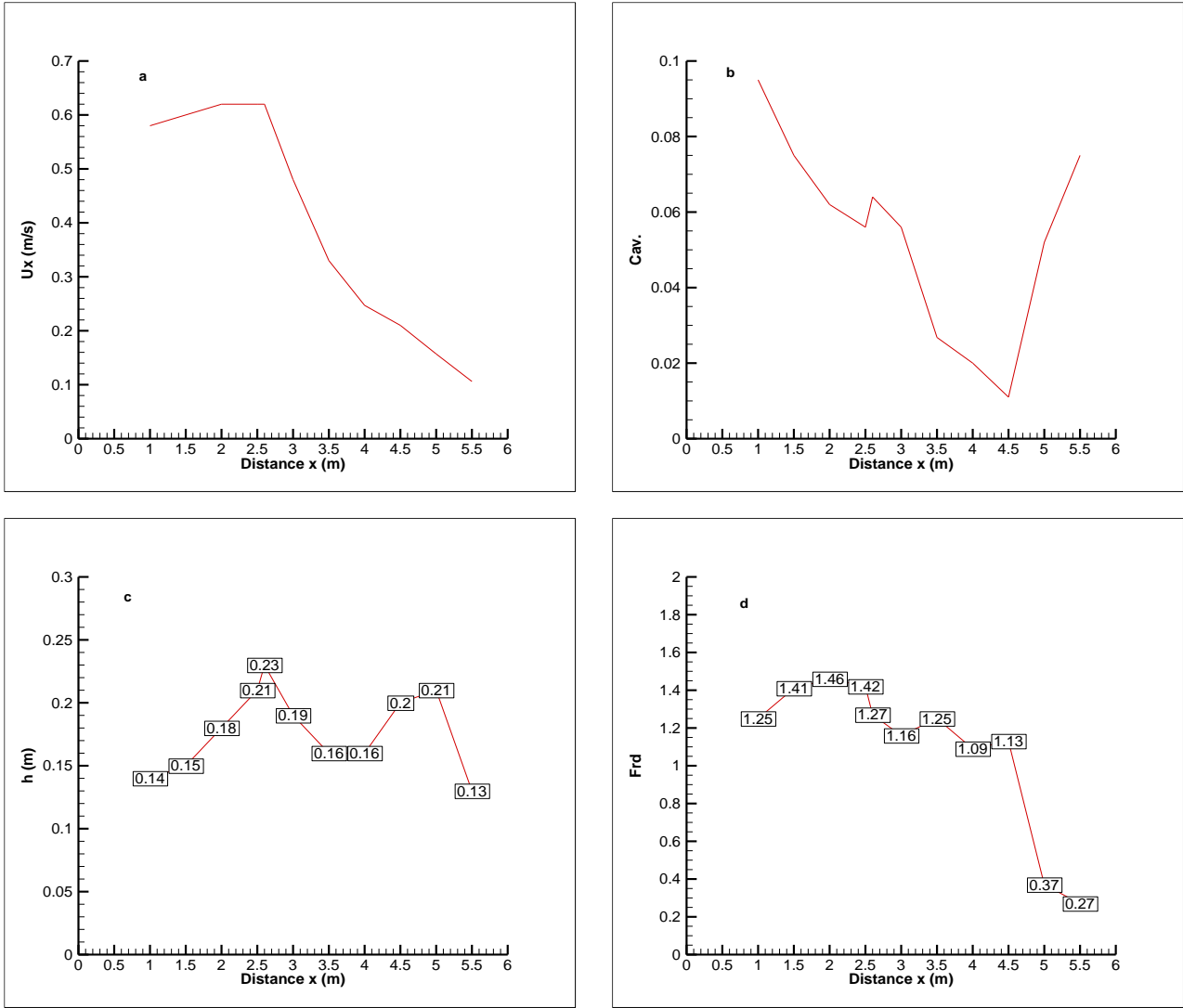


Figure 10: numerical simulation 1, a) Depth averaged x-velocity profile; b) depth averaged suspended sediment concentration (vol.) profile, c) Turbidity current height, d) densimetric Froude number.

The spatial variation of flow dynamics is examined and investigated by plotting x velocity and suspended sediment concentration profiles versus longitudinal distance Figures 17. The velocity is noticed to increase with downstream direction. The largest velocity values occur downstream of the lock gate (Figure 17 a), where most of suspended sediment has been reached (Figure 17 b). The presence of suspended sediment provides the flow with surplus density, which is the flow driving force. The majority of suspended sediment in the current for coarse grains (run G) was still at $x=2.4$ m from the lock gate, whereas suspended sediment in the current for fine grains (run A) had reached $x=3.8$ m.

Figure 17c shows that the near bed suspended sediment concentration longitudinal profiles of runs A, D, and G have a high point within the first 1.2 m of the tank. The concentration then steadily drops with distance beyond the maximum value. Run G has the highest concentration peak, while Run A has the lowest, because large particles with high fall velocities are deposited quickly, allowing

only brief suspension of coarse particles. While fine particles with low fall velocities allow many particles to remain suspended throughout the current propagation time scale.

3.3 Vertical profile and flow structure of Surge Like Turbidity Current

The vertical profiles of velocity and suspended sediment concentration are examined at various times and longitudinal distances to explore the spatial and temporal variations in turbidity current dynamics.

Figures (18) illustrates that the maximum velocity increases with streamwise direction downstream the lock gate for runs A and D at $T=24$ sec. Fine suspended sediments are distributed along the tank in such a way that the amount of suspended sediment near the lock gate ($x=0.5, 1, 1.5$ m) is significantly less than that at the downstream end of the tank ($x=2.5, 3, 3.5, 4$ m), as a result

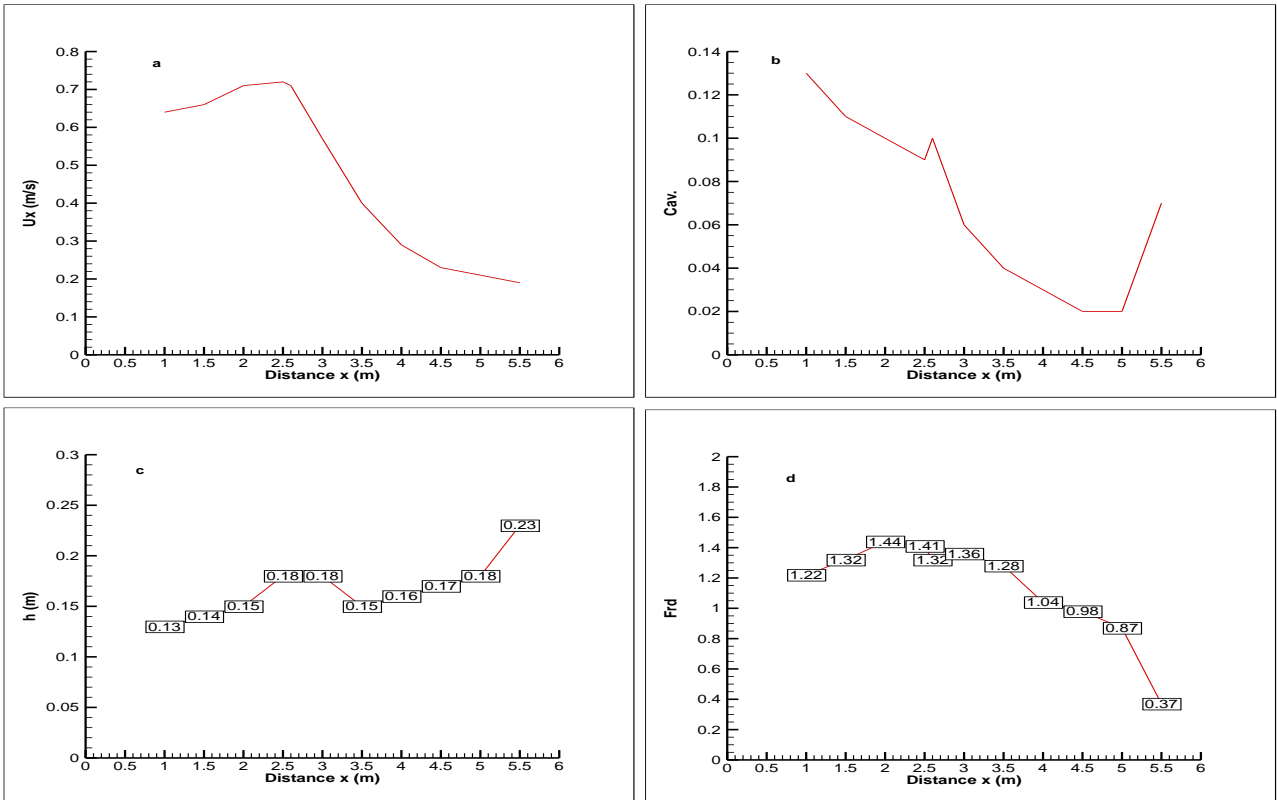


Figure 11: numerical simulation 2, a) Depth averaged x-velocity profile; b) depth averaged suspended sediment concentration (vol.) profile, c) Turbidity current height, d) densimetric Froude number.

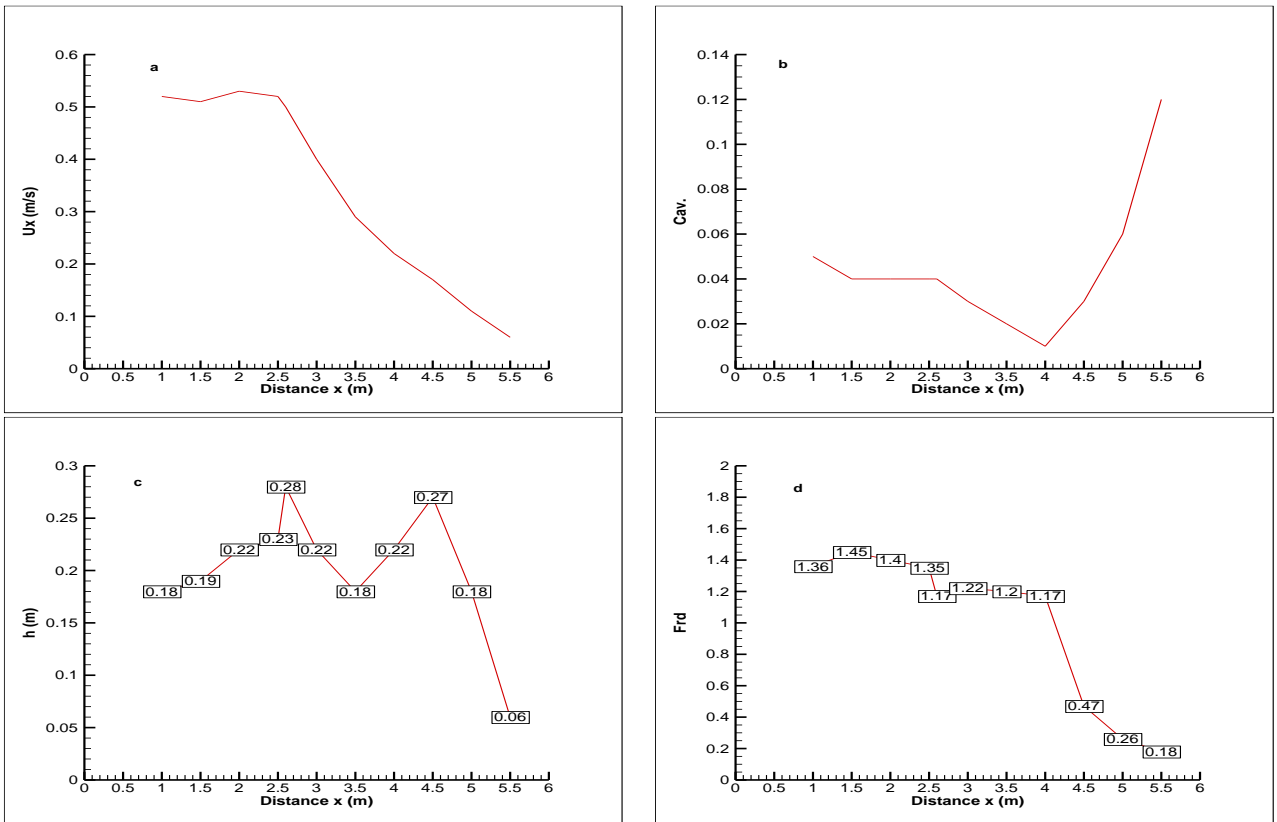


Figure 12: numerical simulation 3, a) Depth averaged x-velocity profile; b) depth averaged suspended sediment concentration (vol.) profile, c) Turbidity current height, d) densimetric Froude number.

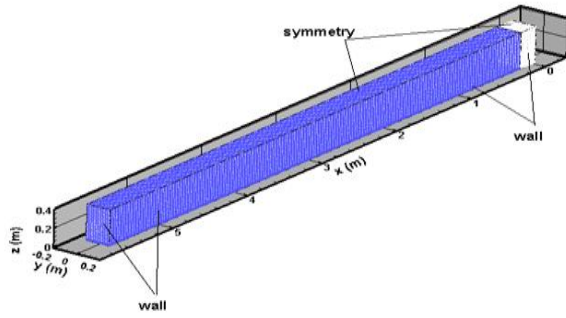


Figure 13: Mesh, geometry, boundary conditions used in numerical model simulating lock gate (C.Gladstone et al.[5])

of continuous translation and settlement of sediment during flow propagation.

As a result, higher velocities occur in the downstream end of the tank due to the presence of higher suspended sediment concentrations, which maintains the flow excess density and, as a result, the flow momentum. Later in flow propagation, the current with coarse grains begins to be manifested as a plume carrying suspended silt, which completely settles out of the flow at the lock gate. This explains the late-time zero velocity data near the lock gate. Time series of the stream wise velocity plots at fixed point are constructed, Figure (19) which is consistent with the vertical x-velocity profiles.

The decrease in velocity with time is caused by a portion of the suspended silt in the turbidity current being convicted and the rest being settled as the flow propagates downstream the lock gate, resulting in a decrease in the flow pushing power.

The vertical distribution of the volumetric concentration profile in figure (20) reveals that finer grains are more equally distributed in the vertical direction because fine grains with low fall velocity are held in suspension by ambient fluid turbulence. While coarse grains are more stratified, with significantly higher near bed concentrations, because coarse grains with high fall velocity deposit more quickly than finer grains. In the body of the turbidity currents, two different layers are produced in all curves: bottom layer with higher density moves parallel to the bed, and an upper more diluted caused by entrainment and mixing of the ambient fluid.

Runs A, D, and G have a peak value for near bed suspended sediment content at all time levels. The maximum near-bed suspended sediment concentration occurs at $x = 1$ m during early flow stages. The maximum near bed suspended sediment concentration occurs at a distance x between 1 and 1.5 m. The observation is interpreted as the turbidity current in run G having coarse grains hence bigger particle size and greater fall velocity generating more deposition than the turbidity current in runs A and D having fine grains with tiny size and slower fall velocity resulting less deposition. At a constant time, the near-bed concentrations of coarser particle size (run G) fall dramatically compared to runs A and D.

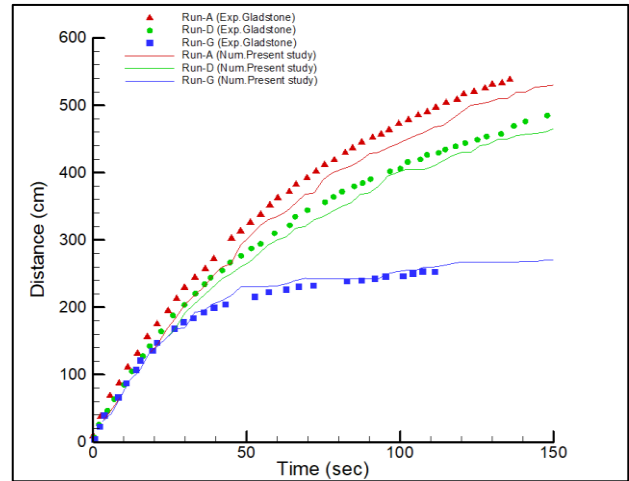


Figure 14: Comparison of numerical model (present study) and experimental results (Gladstone et al.1998), of current front propagation with respect to time

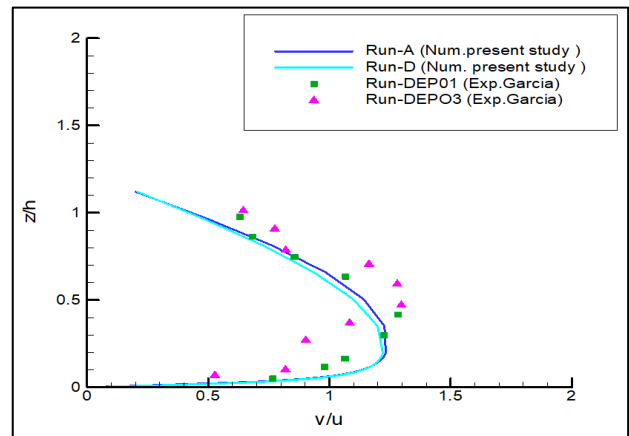


Figure 15: Comparison of numerical dimensionless velocity profile (present study) with experimental results (Garcia 1994) at $x=1$ m, $y=0$ m, and $t=30$ sec

The near bed suspended sediment concentrations at a fixed distance x streamwise the flow direction increase quickly with time, which is attributable to the high deposition rate during early flow evolution. In run A, sediment concentrations gradually grow and then remain constant over time, but in runs D and G, sediment concentrations reach a peak and then gradually decrease and remain practically constant. For runs A near bed suspended sediment concentration steadily increases during the time scale of current propagation. While near bed suspended sediment concentration in run G increases sharply at the beginning of flow evolution, it gradually decreases at the end, indicating a continuous and large deposit rate of coarse particles compared to fine grains at the beginning of flow evolution and a slower deposit rate at the end. The decrease in near-bed suspended sediment concentration for run G at late flow stages could be attributed to sediment resuspension caused by increased shear stress caused by an ambient water back flow wave formed at the interface between dense fluid (turbidity current) and the dilute fluid above.

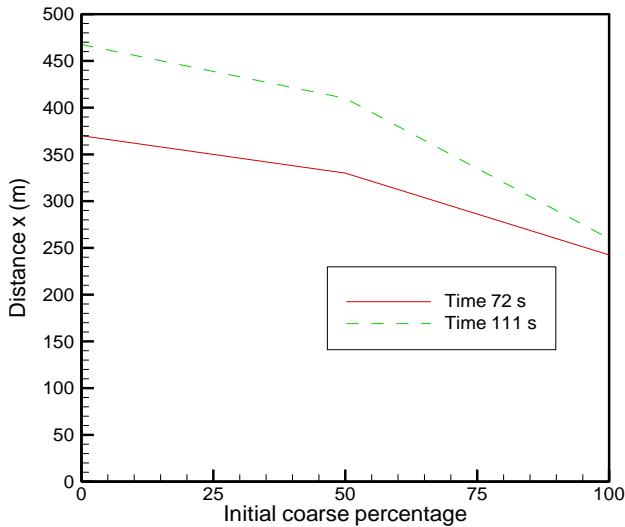


Figure 16: Relationship between distance reached by the current front with respect to initial percent of coarse sediment fraction at fixed times

For runs A and G, time series of suspended sediment concentration contours are created from numerical simulation results. Figure (22) shows that fine and coarse loaded turbidity currents move at the same pace up to $t=18$ sec. Later in evolution, the coarse turbidity current runs at a slower rate than the fine loaded turbidity current, which has a less defined structure. This is because particle deposition rates are higher in coarse-laden flow. It is also observed that the thickness of both currents decreases at later stages of evolution, because of the back-flow wave generated at the interface between turbidity current and ambient water, which moves upstream in the opposite direction of the turbidity current until it hits the lock gate and reflects. Fine and coarse loaded turbidity currents are both subcritical flows along its longitudinal direction. The thickness of turbidity current in Run A decreases with distance downstream lock gate, whereas the depth averaged x-velocity increases with increase in suspended sediment concentration. On the other hand, the x-velocity and thickness of turbidity currents in Run G increase, reaching a peak value at $x=1.5$ m and $x=2$ m, respectively, before decreasing.

4 CONCLUSION AND RECOMMENDATIONS

A 3D multiphase numerical model is adopted to simulate the underflow turbidity currents. The numerical model is calibrated and validated with comparison of two sets of experimental data available in literature. The developed numerical model demonstrates satisfactory match in reproducing experimental data for both Continuous unconfined turbidity current and for surge like confined turbidity current. For continuous unconfined turbidity current it is found clearly from the numerical simulations that, the current possesses a discrete head, two unique body layers, and two velocity layers.

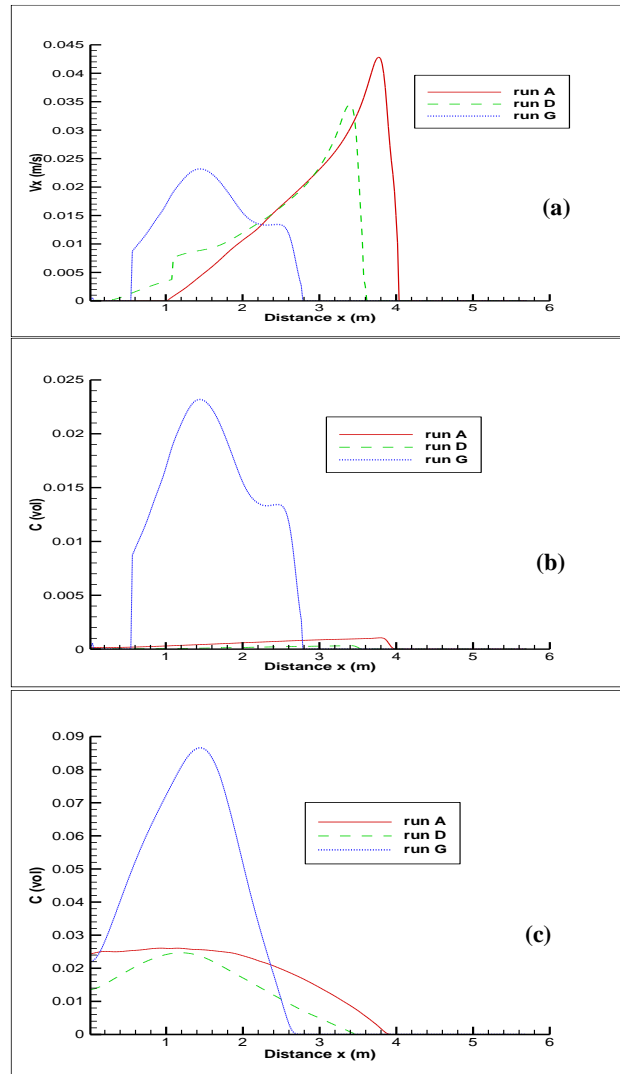


Figure 17: a) Variation of x-velocity in the longitudinal downstream direction, at $t=72$ sec., $z=0.008$ m, $y=0$; b) Variation of suspended sediment concentration in the longitudinal downstream direction, at $t=72$ seconds, $z=0.008$ m, and $y=0$ m, c) Variation of volumetric deposited sediment concentration in the longitudinal downstream direction, at $t=72$ seconds, $z=0.002$ m, and $y=0$ m.

The lower layer at moves more rapidly than the upper layer due to high sediment concentration. Turbidity currents are supercritical on the sloped channel and subcritical at the mild sloped unconfined seafloor or reservoir bottom. The thickness of turbidity currents develops gradually inside confined channels and then reduces abruptly at the entry of unconfined environment causing formation of turbidite submarine fan.

Head velocity of continuous unconfined current is found to be less than the velocity of the current body due to continuous sediment supply into the current body. The opposite is found to occur in surge-like confined current

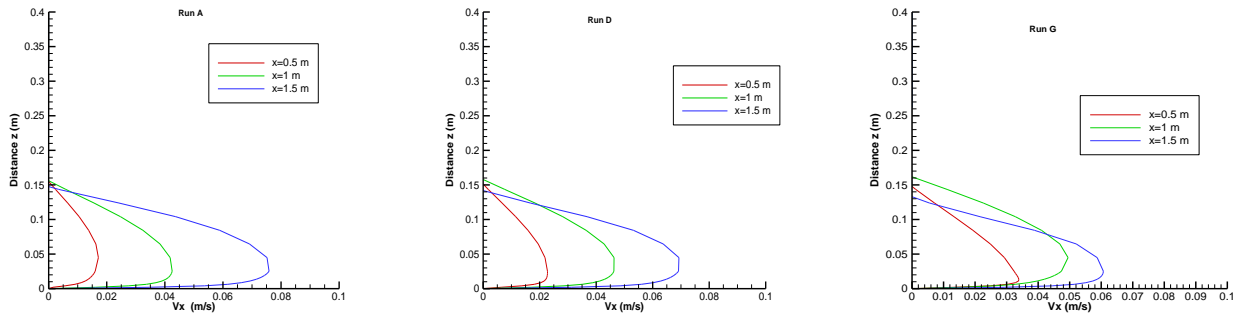


Figure 18: Streamwise Velocity profile at various longitudinal distances for runs A, D, and G, at T=24 seconds and y=0 m.

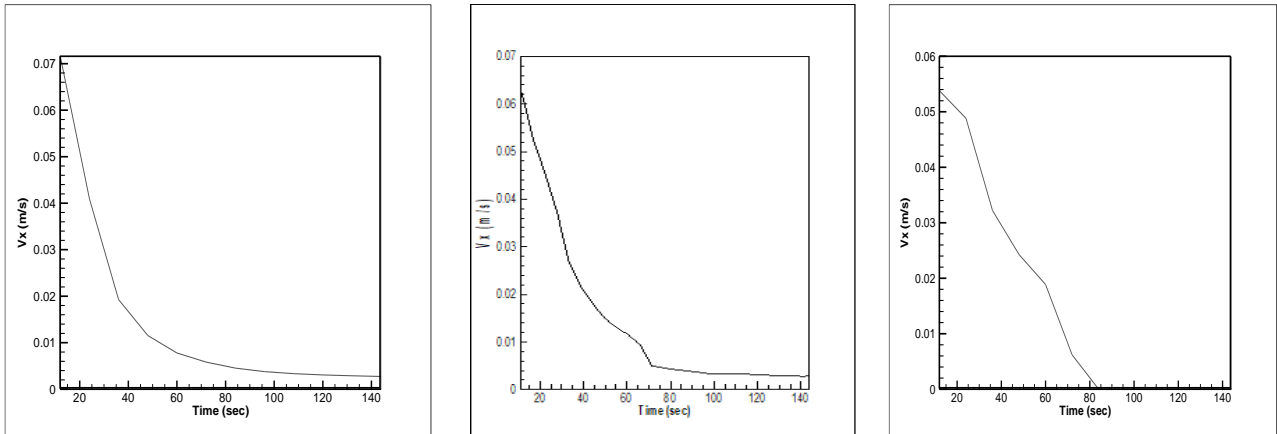


Figure 19: X- velocity Time series for run A, D and G at x=1 m, y=0 m, and z=0.05 m

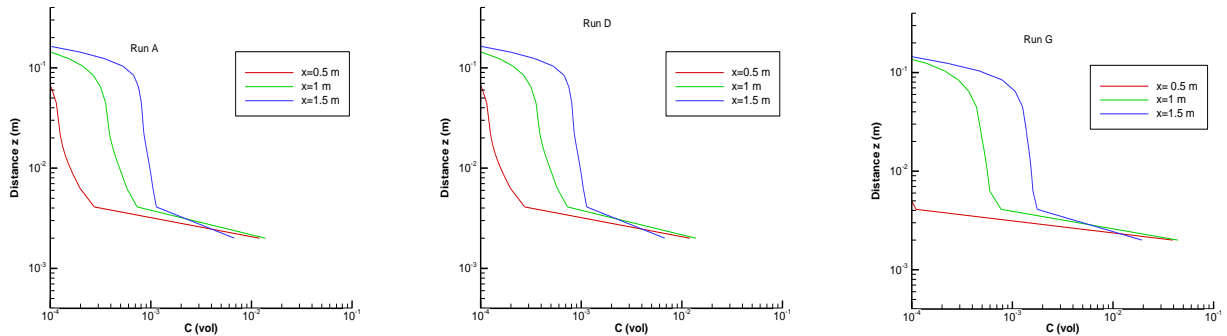


Figure 20: Volumetric concentration profile at various longitudinal distances for runs A, D, G, at T=24 sec., and y=0 m

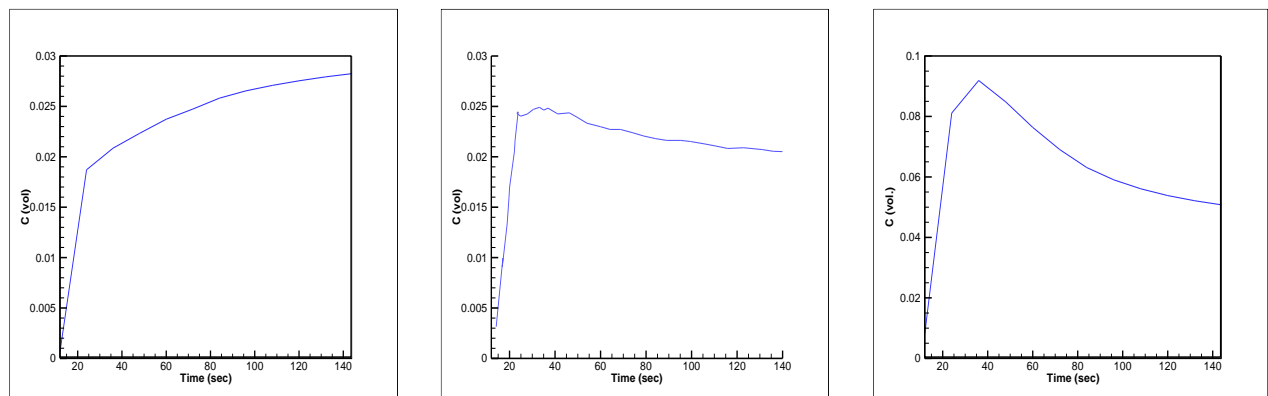


Figure 21: Near bed sediment concentration Time series for run A, D, and G at x=1 m, y=0 m, and z=0.0002 m

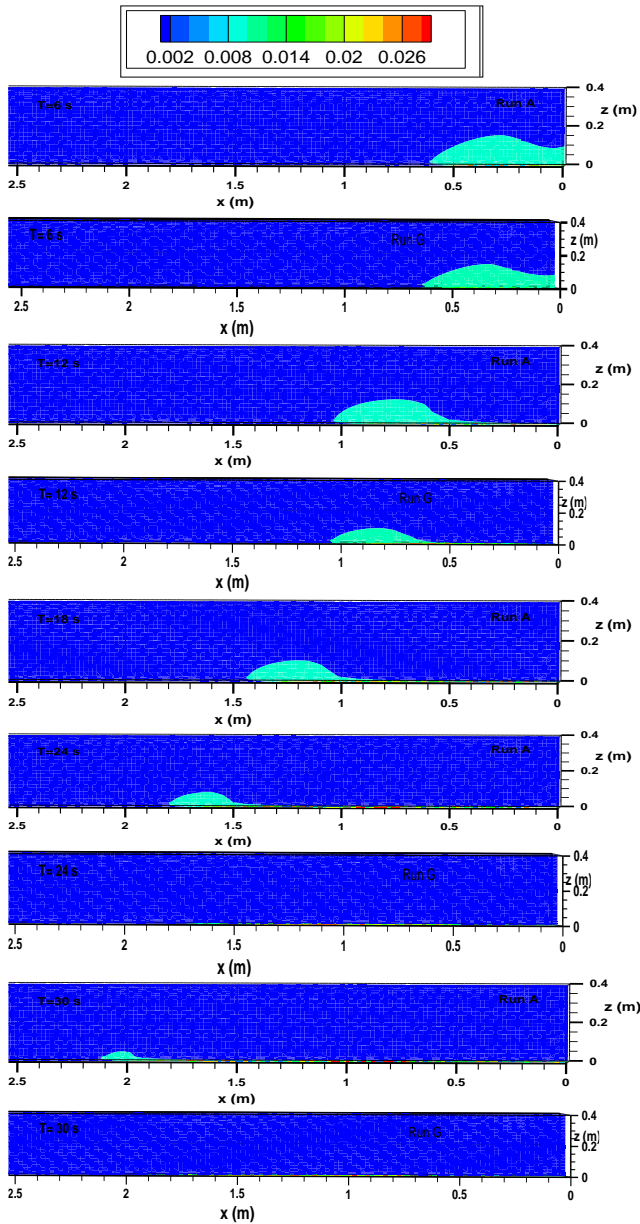


Figure 22: Time series of suspended sediment concentration contours for numerical runs A and G

where the head velocity is larger than the current body velocity due to single release of sediment load and thus higher sediment concentration is found in the current head compared to the current body.

For the surge-like confined current carrying fine sediment, near bed sediment concentration increases with time reaching a constant while for currents carrying coarse sediments, near bed sediment concentration increases reaching a peak value then decreased with time. This is attributed to bed load movement causing reduction in deposition for the current with coarse sediment.

Investigating variation of surge like turbidity current velocity with downstream distance, it is found that the velocity increases with stream wise flow distance but decreases with time at fixed distance. On the other hand,

sediment concentration near bed increases with distance downstream reaching a peak value then decreases, having the highest peak for runs with coarse grains. The thickness of turbidity current increases gradually inside the confined channel then decreases suddenly at the entrance of the unconfined basin due to the horizontal spreading in the basin.

It can be concluded that, the developed numerical model is capable of simulating; confined and unconfined continuous or surge like turbidity currents with reasonable and reliable match. The adopted model can accurately simulate and predict numerous aspects turbidity currents at the field scale and to investigate the dynamics and properties of any type of turbidity current with depositional pattern. The model shall be used to investigate the dynamics and properties of continuous unconfined and surge-like confined turbidity currents through hypothetical simulations at the field scale. This shall be presented in future study.

Acknowledgments

I would like to express my gratitude to the individuals who contributed to this research project. Their insights, feedback, and support were instrumental in shaping the direction of this work. I would also like to acknowledge the participants who generously gave their time to make this study possible. Without their cooperation, this research would not have been possible. Additionally, I am grateful for the resources and facilities that were made available to me during this project. Finally, I would like to thank my loved ones for their unwavering support and encouragement throughout this journey.

Author Contribution:

Tarek M. Salah EL-Din: Methodology, writing original draft, writing-review, supervision, and editing.

Serine A. Bashandy: Software, original draft, Visualization, Investigation.

Competing Interest: The authors declare there are no competing interests.

Funding: The authors declare no specific funding for this work.

5 REFERENCES

- [1] M. G. Wells and R. M. Dorrell, "Turbulence Processes Within Turbidity Currents," *Annu. Rev. Fluid Mech.*, vol. 53, no. 1, pp. 59–83, Jan. 2021, doi: 10.1146/annurev-fluid-010719-060309.
- [2] M. Azpiroz-Zabala *et al.*, "Newly recognized turbidity current structure can explain prolonged flushing of submarine canyons," *Sci. Adv.*, vol. 3, no. 10, Oct. 2017, doi: 10.1126/sciadv.1700200.
- [3] J. Imran, G. Parker, and N. Katopodes, "A numerical model of channel inception on

- submarine fans,” *J. Geophys. Res. Ocean.*, vol. 103, no. C1, pp. 1219–1238, Jan. 1998, doi: 10.1029/97JC01721.
- [4] M. La and A. Batem, “Experimental and Theoretical Modelling of 3D Gravity Currents,” in *Numerical Simulations - Examples and Applications in Computational Fluid Dynamics*, InTech, 2010. doi: 10.5772/13251.
- [5] GLADSTONE, PHILLIPS, and SPARKS, “Experiments on bidisperse, constant-volume gravity currents: propagation and sediment deposition,” *Sedimentology*, vol. 45, no. 5, pp. 833–843, Oct. 1998, doi: 10.1046/j.1365-3091.1998.00189.x.
- [6] M. FELIX and J. PEAKALL, “Transformation of debris flows into turbidity currents: mechanisms inferred from laboratory experiments,” *Sedimentology*, vol. 53, no. 1, pp. 107–123, Feb. 2006, doi: 10.1111/j.1365-3091.2005.00757.x.
- [7] J. H. Baas, W. Van Kesteren, and G. Postma, “Deposits of depletive high-density turbidity currents: a flume analogue of bed geometry, structure and texture,” *Sedimentology*, vol. 51, no. 5, pp. 1053–1088, Oct. 2004, doi: 10.1111/j.1365-3091.2004.00660.x.
- [8] K. M. Straub, “Quantifying turbidity current interactions with topography,” 2007. [Online]. Available: <http://dspace.mit.edu/handle/1721.1/40864>
- [9] R. Cossu and M. G. Wells, “A comparison of the shear stress distribution in the bottom boundary layer of experimental density and turbidity currents,” *Eur. J. Mech. - B/Fluids*, vol. 32, pp. 70–79, Mar. 2012, doi: 10.1016/j.euromechflu.2011.09.006.
- [10] P. R. Hill and D. G. Lintern, “Turbidity currents on the open slope of the Fraser Delta,” *Mar. Geol.*, vol. 445, p. 106738, Mar. 2022, doi: 10.1016/j.margeo.2022.106738.
- [11] T. M. H. Guimarães, D. K. Koller, J. J. Fedele, and R. Manica, “Turbidity currents generating lobes: flow rate influence on 3D experiments without slope break,” *Brazilian J. Geol.*, vol. 52, no. 4, 2022, doi: 10.1590/2317-488920220220029.
- [12] X. Liu, J. Sun, Y. Lu, and X. Guo, “Control of ambient fluid on turbidity current evolution: Mechanisms, feedbacks and influencing factors,” *Geosystems and Geoenvironment*, vol. 2, no. 4, p. 100214, Nov. 2023, doi: 10.1016/j.geogeo.2023.100214.
- [13] R. T. Bonnecaze, H. E. Huppert, and J. R. Lister, “Particle-driven gravity currents,” *J. Fluid Mech.*, vol. 250, pp. 339–369, May 1993, doi: 10.1017/S002211209300148X.
- [14] M. H. Garcia, “Depositional Turbidity Currents Laden with Poorly Sorted Sediment,” *J. Hydraul. Eng.*, vol. 120, no. 11, pp. 1240–1263, Nov. 1994, doi: 10.1061/(ASCE)0733-9429(1994)120:11(1240).
- [15] T. M. Salaheldin, J. Imran, M. H. Chaudhry, and C. Reed, “Role of fine-grained sediment in turbidity current flow dynamics and resulting deposits,” *Mar. Geol.*, vol. 171, no. 1–4, pp. 21–38, Dec. 2000, doi: 10.1016/S0025-3227(00)00114-6.
- [16] G. De Cesare, A. Schleiss, and F. Hermann, “Impact of Turbidity Currents on Reservoir Sedimentation,” *J. Hydraul. Eng.*, vol. 127, no. 1, pp. 6–16, Jan. 2001, doi: 10.1061/(ASCE)0733-9429(2001)127:1(6).
- [17] B. HALL, E. MEIBURG, and B. KNELLER, “Channel formation by turbidity currents: Navier–Stokes-based linear stability analysis,” *J. Fluid Mech.*, vol. 615, pp. 185–210, Nov. 2008, doi: 10.1017/S0022112008003467.
- [18] J. Singh, “Simulation of suspension gravity currents with different initial aspect ratio and layout of turbidity fence,” *Appl. Math. Model.*, vol. 32, no. 11, pp. 2329–2346, Nov. 2008, doi: 10.1016/j.apm.2007.09.032.
- [19] M. Strauss and M. E. Glinsky, “Turbidity current flow over an erodible obstacle and phases of sediment wave generation,” *J. Geophys. Res. Ocean.*, vol. 117, no. C6, Jun. 2012, doi: 10.1029/2011JC007539.
- [20] A. N. Georgoulas, P. B. Angelidis, T. G. Panagiotidis, and N. E. Kotsovinos, “3D numerical modelling of turbidity currents,” *Environ. Fluid Mech.*, vol. 10, no. 6, pp. 603–635, Dec. 2010, doi: 10.1007/s10652-010-9182-z.
- [21] L. Lesshafft, E. Meiburg, B. Kneller, and A. Marsden, “Towards inverse modeling of turbidity currents: The inverse lock-exchange problem,” *Comput. Geosci.*, vol. 37, no. 4, pp. 521–529, Apr. 2011, doi: 10.1016/j.cageo.2010.09.015.
- [22] F. Giorgio Serchi, J. Peakall, D. B. Ingham, and A. D. Burns, “A numerical study of the triggering mechanism of a lock-release density current,” *Eur. J. Mech. - B/Fluids*, vol. 33, pp. 25–39, May 2012, doi: 10.1016/j.euromechflu.2011.12.004.
- [23] S. An and P. Y. Julien, “Three-Dimensional Modeling of Turbid Density Currents in Imha Reservoir, South Korea,” *J. Hydraul. Eng.*, vol. 140, no. 5, May 2014, doi: 10.1061/(ASCE)HY.1943-7900.0000851.
- [24] G. A. Albertão, R. Eschard, T. Mulder, V. Teles, B. Chauveau, and P. Joseph, “Modeling the deposition of turbidite systems with Cellular Automata numerical simulations: A case study in the Brazilian offshore,” *Mar. Pet. Geol.*, vol. 59, pp. 166–186, Jan. 2015, doi:

- 10.1016/j.marpetgeo.2014.07.010.
- [25] M. M. Traer, A. Fildani, O. Fringer, T. McHargue, and G. E. Hilley, "Turbidity Current Dynamics: 1. Model Formulation and Identification of Flow Equilibrium Conditions Resulting From Flow Stripping and Overspill," *J. Geophys. Res. Earth Surf.*, vol. 123, no. 3, pp. 501–519, Mar. 2018, doi: 10.1002/2017JF004200.
- [26] P. Hu and Y. Li, "Numerical modeling of the propagation and morphological changes of turbidity currents using a cost-saving strategy of solution updating," *Int. J. Sediment Res.*, vol. 35, no. 6, pp. 587–599, Dec. 2020, doi: 10.1016/j.ijsrc.2020.05.003.
- [27] H. Naruse and K. Nakao, "Inverse modeling of turbidity currents using an artificial neural network approach: verification for field application," *Earth Surf. Dyn.*, vol. 9, no. 5, pp. 1091–1109, Sep. 2021, doi: 10.5194/esurf-9-1091-2021.
- [28] M. Rakesh, P. K. Rakesh, B. Kumar, S. Chowdhury, and A. K. Patidar, "Numerical simulation of gravity driven turbidity currents using Computational fluid dynamics," *Mater. Today Proc.*, vol. 50, pp. 1883–1891, 2022, doi: 10.1016/j.matpr.2021.09.238.
- [29] R. Zhang, B. Wu, and B. Zhang, "Sensitivity analysis of a three-dimensional simulation of turbidity currents in a sloping flume," *J. Hydraul. Res.*, vol. 61, no. 1, pp. 18–33, Jan. 2023, doi: 10.1080/00221686.2022.2106590.
- [30] J. P. Masterson, "Simulated Interaction Between Freshwater and Saltwater and Effects of Ground-Water Pumping and Sea-Level Change, Lower Cape Cod Aquifer System, Massachusetts," *U.S. Geol. Surv. Sci. Investig. Rep.*, vol. 2004–5014, p. 72, 2004, [Online]. Available: <http://www.usgs.gov/%0Ahttps://pubs.er.usgs.gov/publication/sir20045014>